

Modeling and parametric study of solid oxide fuel cell performance

Mohamed Mankour^{1,2}, M'hamed Sekour^{1,2}

¹Faculty of Technology University Docteur Moulay Tahar Saïda, Saïda, Algeria

²Department of Electrotechnical, Electrotechnical Engineering Laboratory, University Saïda, Saïda, Algeria

Article Info

Article history:

Received Dec 15, 2021

Revised Apr 9, 2022

Accepted Apr 27, 2022

Keywords:

Electrochemical

Fuel cell

Modeling

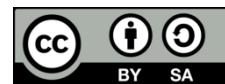
SOFC

Solid oxide

ABSTRACT

Renewable energies are in the news these days and are seen as a solution to endorse energy independence and diminish greenhouse releases. One possible new renewable source that is emerging as a promising technology is the fuel cell. The 'F.C' is an electrochemical system that transfers the chemical power of a redox response into electrical energy with simultaneous production of water and heat. In fact, there are numerous kinds of fuel cells; in our work we are interested in studying the solid oxide fuel cell SOFC. In the context of this work, a modeling tool has been implemented SOFCs to the analogy between the electrical, thermal and chemical domains; this way of proceeding constitutes a simple, evolutionary and efficient tool. Using this modeling, a simulation was carried out in order to obtain the dissimilar characteristics and the impact of the studied parameters on the performance of the SOFC fuel cell.

This is an open access article under the [CC BY-SA](#) license.



Corresponding Author:

Mohamed Mankour

Department of Electrotechnical, Electrotechnical Engineering Laboratory, University Saïda Algeria

Saïda 20000, Alegria

Email: mankourmohamed312@yahoo.fr

1. INTRODUCTION

In recent decades, solid oxide fuel cell SOFCs cells have attracted a lot of attention, owing to their potential uses as stationary power producers and mobility (ground, marine, air). The great energy conversion efficiency and minimal hazardous emission levels of SOFCs make them appealing (only the CO₂ released by the hydrogen production process is a concern). Modularity, fuel flexibility, and minimal noise are among the other benefits [1]-[3]. Furthermore, high operating temperatures afford good features, such as potential utilize of SOFCs in extremely proficient cogeneration applications. Solid oxide fuel cells are also appropriate for internally reforming the fuel (e.g. natural-gas, propane, methanol, gasoline, and diesel), as a result making it doable to stay away from the acceptance of both highly sophisticated, expensive outside reformer and to remove the complexities from fuel storage [4]. The giant confronts to promote the dispersion of SOFC-based energy conversion systems are mostly connected to manufacture costs and permanence. The accomplishments of these objectives shall definitely contribute to upholding the technology and lastly beginning a mass production stage. Above and beyond expenses and performance, long-standing steadiness is a crucial condition for the marketable application of the SOFC technology [5], [6].

The hydrogen vector, namely fuel cells and electrolysis (to make hydrogen), also offers promising potential for these large-scale storage applications, where conventional batteries play a key role. As a result, the storage solution will be multi-system, and the electrical study of the association of many sources of energy - hybridization - will take on new significance in this context. Solid oxide fuel cells (SOFC) are electrochemical devices that allow chemical energy to be converted into electrical energy. The premise is straightforward: water and electricity are produced from a fuel like hydrogen and an oxidant like oxygen.

Apart from the fact that these systems are environmentally friendly since they do not emit greenhouse gases, they also show the potential of hydrogen as an energy vector for both the production of electricity and the storage of energy in chemical form. The applications primarily pertain to decentralized energy generation for residential and urban regions with electrical powers ranging from a few kW to a few hundred kW over hundreds of hours [7], [8]

2. OPERATING MODEL OF SOFC CELL

Cell is a set of an anode, an electrolyte, a cathode and the interconnections. The anode is supplied with hydrogen or gas mixture (fuel) and the cathode is supplied with air (oxidizer). The operating principle of the SOFC is hinged on the following mechanism: oxygen is dissociated at the cathode into O_2^- , then the cation migrates through the ionic conductive electrolyte at high temperature (from 700 °C) and will combine at the anode with hydrogen to form water and release electrons that go via an outsider electrical circuit [8]-[10]. The main characteristic of SOFC is therefore their operating temperature (600 to 1,000 °C), which is mandatory to obtain an adequate ionic dynamism of the ceramic electrolyte. This temperature has a double advantage. Firstly, it allows the direct use of hydrocarbons, which can be easily reformed without the need for a noble metal catalyst. Secondly, it produces a high level of heat that can be easily used in cogeneration, with an efficiency of up to 80%.

But it also has a disadvantage; the heating is long and complicates any use with short and repetitive cycles (as in the case of transport). For these reasons, the technology lends itself particularly well to decentralized electricity production and cogeneration (areas covering powers ranging from 1 KW to several tens of MW) [11]-[13]. Thanks to its high efficiency and its potential capacity to operate directly with liquid hydrocarbons, it will also find an outlet in naval propulsion. The development of this type of cell, because of its high operating warmth and the resolution of thermo-mechanical problems of material resistance, is quite complex. One of the particularities of the SOFC is its solid electrolyte, usually zirconium (Zr_2) doped with a mole of 8 to 10% yttrium (Y_3^+), which acts as a conductor for the oxygen anion (O_2^-). The following Figure 1 shows the operating principle of the SOFC fuel cell.

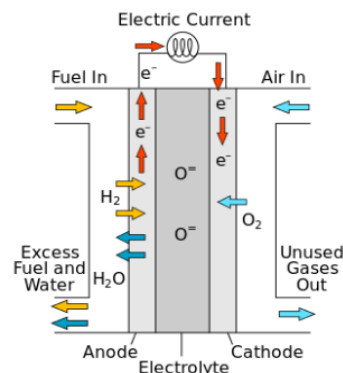


Figure 1. Picture of SOFCs

3. POLARIZATIONS

Polarizations, or overvoltage's, are voltage losses as consequence of drawbacks in the structure of the F.C polyanionic cellulose (PAC) and materials microstructure. The ohmic confrontation of 'oxyg' ions passing through the electrolyte ($i.R \Omega$), electro_chemicals activated hurdles at the 'ano' and 'cath', and terminaly focus polarizations in view the incapacity of gas's to distribute at high velocities through the porous anode and cathode [10]. The cell voltage can be calculated employing in (1):

$$\text{Volt} = E_0 - R * i - \eta_{cathode} - \eta_{anode} \quad (1)$$

In SOFC, it is frequently essential to spotlight on Ohmic and attentiveness biases because high operating heats background little's activation polarizations. Nonetheless, like the lowest boundary of the S.O.F.C functioning hotness is came close to (~873,15 kelvin), these polarizations turn out to be significant. Research by Huo [14] The above equation is utilized to find out the S.O.F.C voltage. This method showed results which gives a excellent accord with scrupulous investigational Information and deprived agreement for

experimental working parameters other than the originals. Additionally, most of the equations employed need the addition of multiple factors that are hard or unfeasible in order to identify. This that any process of optimizing the S.O.F.C operating fact and the choosing very complicated geometry configuration. Because these circumstances, a few other equations have been suggested [15].

$$E_{SOFC} = \frac{E_{max} - i_{max} \cdot \eta_f \cdot r_1}{\frac{r_1}{r_2} (1 - \eta_f) + 1} \quad (2)$$

Where:

- E_{SOFC} : Cell voltage
- E_{max} : The Nernst equation predicts the maximum voltage
- i_{max} : Current density at its maximum (for a given fuel flow)
- η_f : Factor of fuel usage [15], [16]
- r_{-1} : The electrolyte's particular ionic resistance
- r_{-2} : The electrolyte's particular electrical resistance

4. THE LOSSES SOFC MODEL

There are three main forms of polarization overvoltage's: activation, ohmic and concentration. A constant offset also contributes to the total polarization, resulting from small overvoltages like contact resistor, inside currenty and leakage. According to [17], the shift was approximated to be 0.07 volts. the additions of the different polarizations result in a voltage sag from the optimal Nernst potential to the actual working value. As the interconnector and the electrodes are iso-polar, the array voltage is constant over the cell and can be expressed in (3):

$$V_{SOFC} = E_{Nernst}^i - V_{Act}^i - V_{Ohm}^i - V_{Con}^i - V_{Offset}^i \quad (3)$$

The total energy derived from the S.O.F.C is determined as shown in (4):

$$E_{Cel} = V_{SOFC} \cdot I_{SOFC} \quad (4)$$

4.1. Activation polarization

'Activ' polarization means the power obstacle being diminished in order to enable the electro_chemical feedback taking part at the interface of the electrodes [18]. This quantity of power unavoidably leads to a noteworthy overvoltage, that is typically modelled by the non-linear equation recognized as butler-wolmer formula [19]:

$$V_{Act}^i = \frac{R \cdot T_s^i}{\alpha (T_s^i) \cdot F} \left(\sinh^{-1} \left(\frac{J^i}{2 J_0 (T_s^i)} \right) \right) \quad (5)$$

where α is the charge transmit coefficient and J_0 is the switch present mass.

4.2. 'Ohm' polarization

'Ohm' polarization primarily relies on the ionic momentum of electrodes and the electronic momentum of an electrolyte. Such over voltages are assessed finalizing the content of every part of the S.O.F.C, as (6):

$$V_{Ohm,k}^i = \frac{l_k}{\sigma_k (T_s^i)} \cdot J^i \quad (6)$$

$$V_{Ohm}^i = \sum V_{Ohm,k}^i \quad k = [ano, cath, el]$$

The conductances are approximated with, suggestions in the review of literature [17] for 2nd edition ceramic 'S.O.F.C' stacks, in which the 'ano', 'cath' and 'el' cover materials are nickel cermet, strontium-doped lanthanum manganite and yttrium oxide cured zirconia, correspondingly:

$$\begin{aligned} \sigma_{an} &= 10^3 \\ \sigma_{ca}(T_s) &= c_{-1}(T_s^i)^2 - c_{-2}(T_s^i)^2 - c_{-3} \\ \sigma_{el}(T_s) &= c_{-4}(T_s^i - 273.15)^2 + c_{-5}(T_s^i - 273.15) + c_{-6} \end{aligned} \quad (7)$$

4.3. Concentration polarization

As the relative stresses of hydrogen and oxygen at the ‘ano’ and ‘cath’, respectively, drop as fuel is depleted. The rate of depletion is determined by the cell's average current density. When a result, as a current thickness rises, the relative stresses fall, and a deficiency number re-agents is eventually carried to the electrodes. Until the voltage is decreased to [20], [21], considerable losses occur. ‘Ano’ and ‘cath’ restrict currents are the values at which this phenomena occurs. Concentration polarization is the term for the voltage loss that occurs at high current densities and can be calculated as (8).

$$V_{Con}^i = -\frac{RT_s^i}{2.F} \cdot \left[\frac{1}{2} \ln \left(1 - \frac{J^i}{J_{cs}} \right) + \ln \left(1 - \frac{J^i}{J_{as}} \right) - \ln \left(1 + \frac{P_{H_2}^i \cdot J^i}{P_{H_2O}^i \cdot J_{cs}} \right) \right] \quad (8)$$

The ‘ano’ and ‘cath’ limiting currents are determined as a function of the species scattering coefficients, using the formula given in [22].

5. MODELING OF THE SOFC

The purpose of this paper is to give the model adopted to account for the physical phenomena in the cell. The first part of the paper is dedicated to the modeling principles applied to the chemical, thermal and electrical domains. The second part concerns the application of the modeling to the S.O.F.C Cell. The chemical & thermal modeling of the ‘F.C’ is based on their formal analogy with the electrical domain. The temperature is similar to the voltage and the heat flow is similar to the current. Two heat sources within the cell are considered: endothermic or exothermic heat sources produced by chemical reactions and Ohmic heat sources. Furthermore, pressure is similar to voltage and flow is similar to current. The application of this analogy offers the possibility of representing physical laws within a system with electrical circuits. The use of such a representation allows the use of different techniques in the electrical domain: putting chemical and thermal models in series or in parallel, realization of the regulation of chemical or thermal quantities with the help of methods used in automation (ex: pole compensation), ease and flexibility of integration of developed models in a global model (battery coupling or battery associated with the converter) The electrical model translates the electrochemical phenomena of each cell. The electrical model of the SOFC is based on the reversible Nernst voltage and the different voltage drops.

5.1. Electro-chemical system

We will choose a static SOFC system based on thermodynamics and electrochemical reactions to determine the electrical characteristics of the fuel cell. In a second step we vary the parameters and observe the variation [23]:

$$(\Delta G = \Delta H - T\Delta s) \quad (9)$$

$$(\Delta H = \Delta U + \Delta PV) \quad (10)$$

$$(\Delta U = \omega + \varphi) \quad (11)$$

Δv : Growth in size, ΔU : Internal energy changes, ω : labour, φ : thermal.

$$(\Delta G = \omega + \varphi + P\Delta V - T\Delta s) \quad (12)$$

$$(Q = T\Delta s) \quad (13)$$

$$(\Delta G = \omega + P\Delta V) \quad (14)$$

(-P ΔV), thus:

$$(\Delta G = -n\Gamma\epsilon. -P\Delta V + P\Delta V) \quad (15)$$

As a result, it was simply:

$$(\Delta G = -n\Gamma\epsilon.) \quad (16)$$

With:

ϵ : electromotive strength of the stack, Γ : Constant of Faraday, n : number of electrons transported.

$$\Delta G_r = G_{H_2O} - G_{H_2} - \frac{1}{2} G_{O_2} \quad (17)$$

$$\Delta G_r = G_r - NRT \log \frac{P_{O_2}^{\frac{1}{2}} P_{H_2}}{P_{H_2O}} \quad (18)$$

$$P_{O_2}, P_{H_2}, P_{H_2O}$$

$$E = E^0 + \frac{RT}{nF} \log \frac{P_{O_2}^{\frac{1}{2}} P_{H_2}}{P_{H_2O}} \quad (19)$$

5.2. Real potential of the stack

The survoltages happened because of the shedding of non-reversible load, also named, which are polarization of 'activ', 'Ohm' polarization & 'conc'. High-temperature fuel cells are able to generate enough heat to power the vaporiser, to power the steam generator. This will produce a hydrogen-rich reformate which is then which is then supplied to the cell.

$$V = E - \text{losses} \quad (20)$$

5.3. Capacity and quality requirements

When the temperature of the battery drops, the variance of free energy increases, hence the standard voltage of a stack is in relation to the change in its standard free energy [24].

For water produced in a liquid state at 25 °C, it is:

$$\Delta G_r = -237,190 \text{ joul/Mol.}$$

$$\Delta H_r = -285,840 \text{ joul/Mol.}$$

The Rated stack Voltage is:

$$E_0 = -\frac{\Delta G}{nF} = 122.9 \text{ V}$$

$$\Delta G_r = -228,590 \text{ j/Mol.}$$

$$\Delta H_r = -241,830/\text{mol} \Rightarrow E_0 = 11.8 \text{ V.}$$

However at 1000 °C [25].

$$\Delta H_{1000^\circ C} = \Delta H_{25^\circ C} + \int_{25}^{1000} \Delta C_p dt \quad (21)$$

$$\Delta S_{1000^\circ C} = \Delta S_{25^\circ C} + \int_{25}^{1000} \frac{C_p}{T} dt \quad (22)$$

$$\Delta G_{1000^\circ C} = \Delta H_{1000^\circ C} - T \Delta S_{1000^\circ C} \quad (23)$$

In this scenario, the start signal voltage is: $V_0 = 0.935$ volt.

5.4. Performance of the cell

The chemical reaction is followed by a change in entropy, which leaves a free enthalpy, which may be transformed into work, in this case electrical energy, with the remainder being converted into heat during the chemical reaction in the stack. The report of the free enthalpy on the standard enthalpy of the reaction of water formation corresponds to the performance thermodynamics for a reversible transformation:

$$\Gamma \frac{\Delta G^0}{\Delta H^0_{max}} \quad (24)$$

This performance ranges from 83 percent for liquid water creation to 95 percent for water formation in gaseous forms under typical conditions, but above 10³ °C, the theoretical performance is:

$$\mu_{th} = 0.7337\%$$

a. The voltaic performance [24]-[26]:

Of the in (24) one can define a voltaic performance to performance by voltage:

$$\mu_E = \frac{V_c(I)}{E^0} \quad (25)$$

b. The electrical performance:

It is motivating to describe the notion of electrical performance:

$$\Gamma_{\text{électrique}} = \Gamma E \frac{\Delta G^0 V_c(I)}{\Delta H^0 E^0 \max} \quad (26)$$

$$E \frac{\Delta G^0}{nF \max}$$

$$\Gamma_{\text{électrique}} = \frac{V_c(I)}{E^0} \quad (27)$$

It is then possible to directly measure this electrical performance experimentally using a voltage measurement, or to plot the electrical performance to T Constant by drawing the characteristic V(I) returns. Because this performance is highly dependent on temperature, it is necessary to recalculate E_{\max} for each temperature [27]:

$$\Gamma_{\text{Fonctionnement}} = \frac{V_c(I)}{E_{\text{vide}}} = \frac{V_c(I)}{V_c(0)} \quad (28)$$

6. SIMULATION OF THE SOFC

Simulation and mathematical models shall undoubtedly help in the development of a variety of power generators. But they are even more important in the development of fuel cells. Simulation of these cells allows you to focus on experimental research and improve the accuracy of interpolation and extrapolation of the results. In addition, mathematical models serve as a valuable tool for the design and optimization of fuel cell systems. Simulations are run on different systems with different software packages [28]-[30]. The following Table 1 shows the simulation parameters.

Table 1. The SOFC model values [30]

Settings	Data	Available units
Nominal power	15,000	Watt
Number of Stack	384.00	/
'Ano' forces	2,280.006	Torr
'Cath' forces	2,280.006	Torr
fuel airflow	0.0012	Mol/s
combustible Water rate	0.00001	Mol/s
combustible Hydrogen rate	0.00009	Mol/s
T fuel	799.85	°C
T air	799.85	°C
Current Density	60.00	A/cm ²
V_{out}	440.00	Volt

7. RESULTS AND DISCUSSION

In our study by using a simulation model with block diagrams under simulink Matlab to obtain the electrical and electrochemical characteristics of the SOFC type fuel cell, and then we varied the parameters of the effect of temperature and the effect of gas pressure, the results are the following:

In order to verify the performance of the fuel cell generation system under normal operating conditions, the previously established model was simulated in the MATLAB/Simulink software environment. MATLAB/Simulink software environment. For this simulation, the model was planned With the parameter values extracted from the literature together with experimental data, the results are presented in the following and the interpretation is just after the presentation of the figures.

7.1. Polarization curve

A polarization curve for the SOFC fuel cell is shown in Figures 2 and 3. The characteristic begins with a no-load voltage at zero current, as can be shown. A dramatic reduction in voltage is noted when the cell current increases. The loss of activation voltage and parasites produced by the pace of the electrochemical process create this reduction in cell voltage. The non-linear activation losses contribute to the V(i) curve's downward tendency at low current densities. The activation losses remain the most significant in absolute terms. The Ohmic loss generated by the electrical resistances of the cell causes an almost linear drop in cell voltage and an increase in current above specific values [31]-[33].

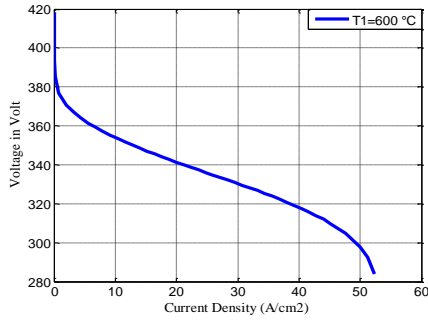


Figure 2. Current-voltage characteristic of a fuel cell SOFC

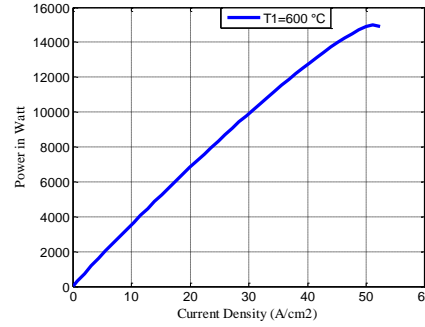


Figure 3. Current-power characteristic of a fuel cell SOFC

7.2. Temperature effect

In this part we have varied the temperature for several values ($T=600\text{ }^{\circ}\text{C}$, $700\text{ }^{\circ}\text{C}$, $800\text{ }^{\circ}\text{C}$, $900\text{ }^{\circ}\text{C}$, $1000\text{ }^{\circ}\text{C}$) and we fix the partial pressure. Figures 4 and 5 show figures at various temperatures typical of SOFCs. The activation voltage drop dominates the voltage drop in the low current region (Figure 6). As the load current increases, the resistance voltage drop increases rapidly and is the main cause of the SOFC voltage drop (Figure 7). At certain load currents, the centralized voltage drop in the SOFC reduces the output voltage of the fuel cell Figure 8. Figure 4 also demonstrates the effect of temperature on SOFC-VI characteristics. The SOFC output voltage is high at low temperatures in the low current region and high at high temperatures in the high current region. From this figure, we can see that rising the cell temperature has a beneficial effect on the cell voltage. This is explained by the high ionic conductivity of the cells (electrolytes and electrodes) at high temperatures (such as $T=900\text{ }^{\circ}\text{C}$, $T=1000\text{ }^{\circ}\text{C}$) Figure 4. Therefore, it is needed to raise the temperature to ensure proper cell function [34], [35]. Tables 2 show the power values according to the influence of temperature:

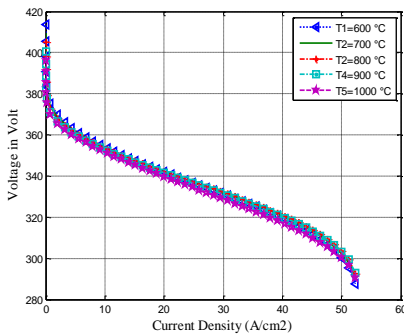


Figure 4. Current-voltage characteristics for different temperatures values

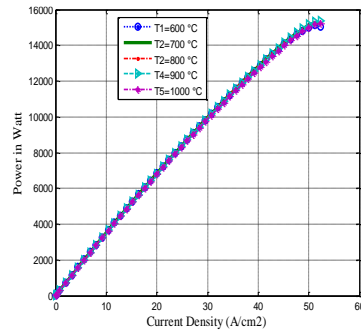


Figure 5. Current-power characteristics for different temperatures values

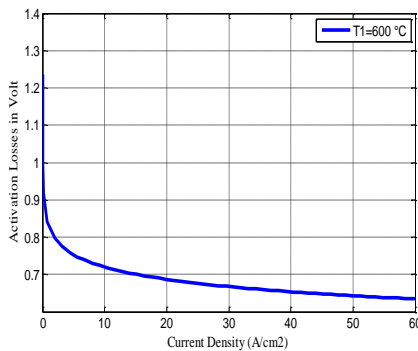


Figure 6. Activation losses characteristics for different temperatures values

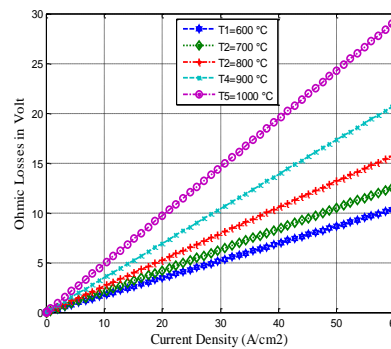


Figure 7. Ohmic losses characteristics for different temperatures values

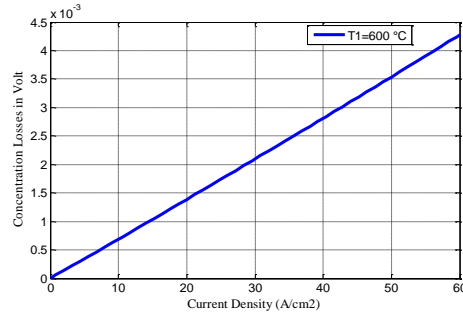


Figure 8. Concentration losses characteristics for different temperatures values

Table 2. Influence of temperature on power

T (°C)	Power (Watt)	Ohmic Losses (Volt)	Activation Losses (Volt)	Concentration Losses (Volt)
600	15,120	10.38	0.6345	0.001938
700	15,25	12.58	/	/
800	15,32	15.8	/	/
900	15,35	20.8	/	/
1000	15,22	29.15	/	/

7.3. Pressure effect

a. Variation of H2 pressure

In this case the temperature is fixed at T=1000 °C and the partial pressure of the H2 gas is varied for the following values (PH2=0.01 Atm, 0.02 Atm, 0.03 Atm) the results are the following. The polarization, activation, Ohmic resistance, and concentration-to-voltage curves at various pressures at 800 °C are shown in Figures 9, 10, 11, 12, and 13, respectively. In the event of a flooding failure, the pressure effect corresponds to the hydrogen and oxygen measured at the fuel cell inlet.

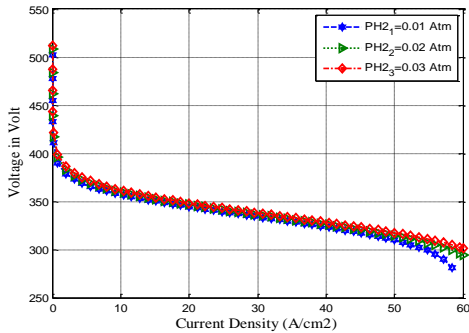


Figure 9. Current-voltage characteristics for different pressures H2 values

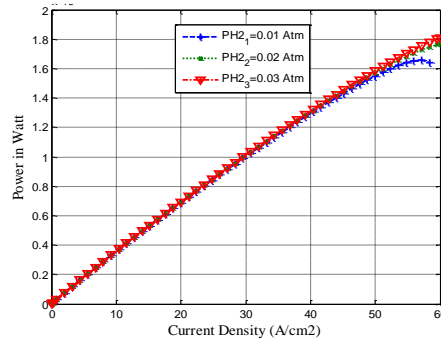


Figure 10. Current-power characteristics for different pressures H2 values

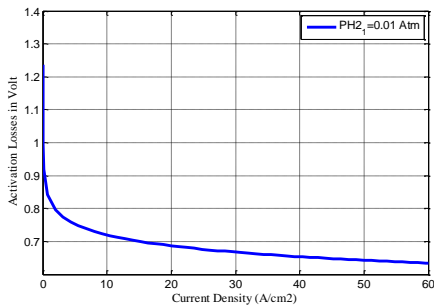


Figure 11. Activation losses characteristics for different pressures H2 values

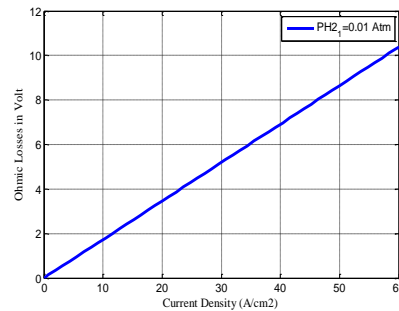


Figure 12. Ohmic losses characteristics for different pressures H2 values

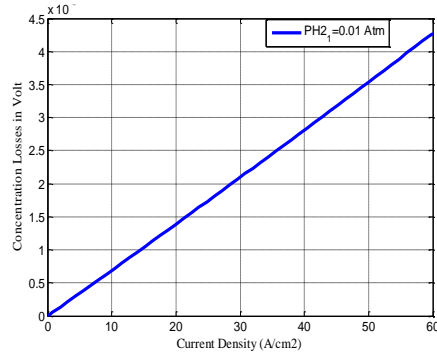


Figure 13. Concentration losses characteristic for different pressures H₂ values

b. Variation of O₂ pressure

In this case the temperature is fixed at T=1000 °C and the partial pressure of the O₂ gas is varied for the following values (PO₂=0.01 Atm, 0.02 Atm, 0.03 Atm) the results are the following. As shown in Figures 14, 15, 16, 17 and 18, as the pressure of oxygen increases, the activation loss decreases and the increasing current density decreases. In addition, increasing pressure reduces concentration loss and increases current density.

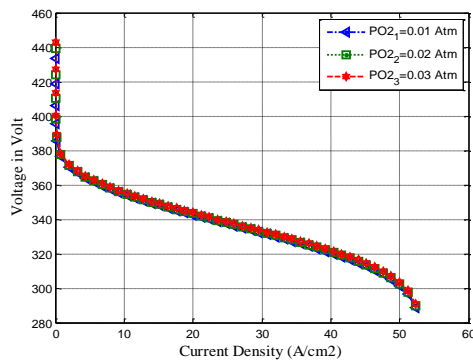


Figure 14. Current-voltage characteristics for different pressures O₂ values

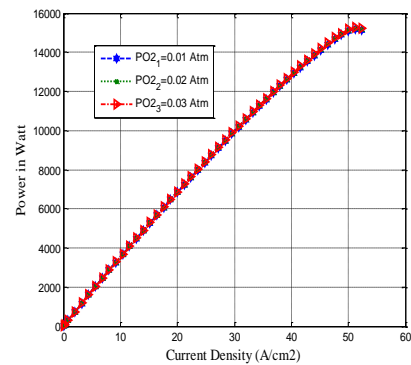


Figure 15. Current-power characteristics for different pressures O₂ values

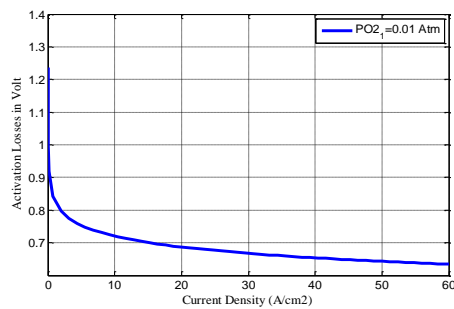


Figure 16. Activation losses characteristics for different pressures O₂ values

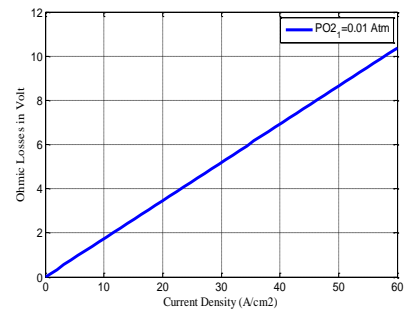


Figure 17. Ohmic losses characteristics for different pressures O₂ values

c. Variation of H₂O pressure

In this case the temperature is fixed at T=1000°C and the partial pressure of the H₂O gas is varied for the following values (PH₂O=0.1 Atm, 0.2 Atm, 0.3 Atm) the results are the following. As shown in Figures 19, 20, 21, 22, and 23. In general, increasing the inlet pressure increases the fuel cell voltage and power density,

as shown in Figure 19. In normal operation of the cell, this pressure is maintained at 1 atmosphere. During the flood condition, the pressure at the inlet will automatically increase, causing cell failure. Therefore, reliable operation of the cell requires efficient monitoring of the cell. Tables 2 to 5 show the power values according to the influence of the pressure for H₂O, O₂, and H₂. From the table, we can see that the value of power rises with the increasing temperature, and the parameter affecting this increase is Ohmic loss. After changing the pressure, you can see that the ohm loss and activation loss, and the concentration remain constant. The result was interpreted after the illustration of all figures.

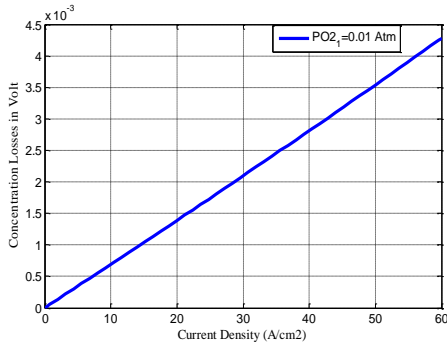


Figure 18. Concentration losses characteristics for different pressures O₂ values

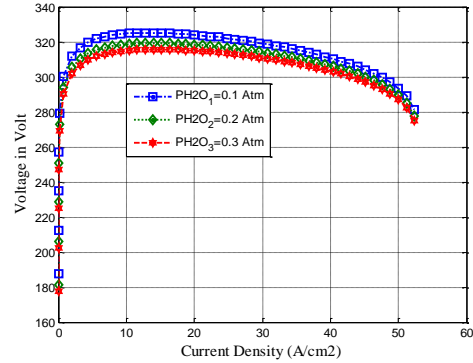


Figure 19. Current-voltage characteristics

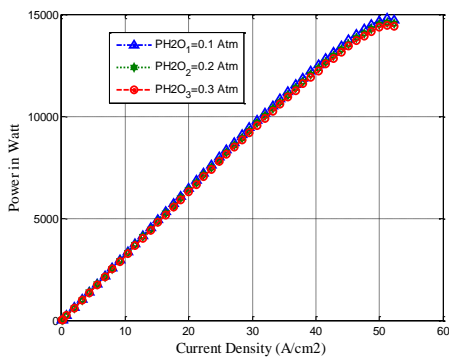


Figure 20. Current-power characteristics for different pressures H₂O values

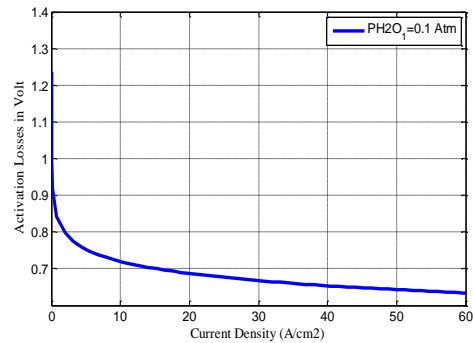


Figure 21. Activation losses characteristics for different pressures H₂O values

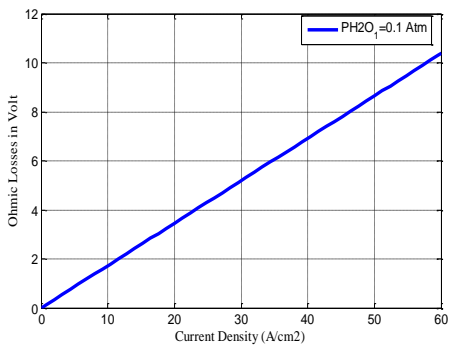


Figure 22. Ohmic losses characteristics for different pressures H₂O values

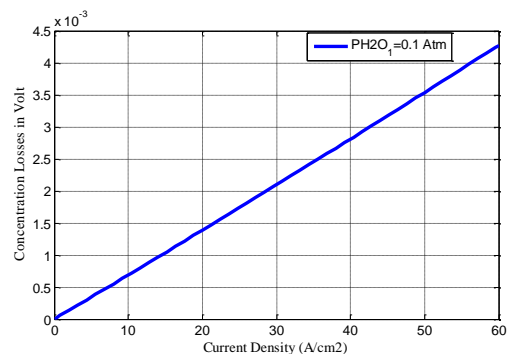


Figure 23. Concentration losses characteristics for different pressures H₂O values

Table 3. Influence of pressures (H₂) on power

P _{H₂} (Atm)	Power (Watt)	Ohmic Losses (Volt)	Activation Losses (Volt)	Concentration Losses (Volt)
0.01	21,150	10.38	0.6345	0.004275
0.02	21,410	/	/	/
0.03	21,630	/	/	/

Table 4. Influence of pressures (O₂) on power

P _{O₂} (Atm)	Power (Watt)	Ohmic Losses (Volt)	Activation Losses (Volt)	Concentration Losses (Volt)
0.01	17,540	10.38	0.6344	0.004275
0.02	17,340	/	/	/
0.03	17,120	/	/	/

Table 5. Influence of pressures (H₂O) on power

P _{H₂O} (Atm)	Power (Watt)	Ohmic Losses (Volt)	Activation Losses (Volt)	Concentration Losses (Volt)
0.1	14,790	10.38	0.6344	0.004275
0.2	14,600	/	/	/
0.3	14,460	/	/	/

8. CONCLUSION

In the context of this work, a macroscopic modelling tool has been implemented thanks to the analogy between the electrical and thermal domains. This method constitutes a simple, scalable and efficient modelling tool. Once the component library has been completed, we will have a complete tool for studying and optimising the architecture of fuel cell systems, taking into account the different energy flows: electrical and thermal. Finally, we look at cogeneration systems using solid oxide fuel cells (SOFC).

As explained above for a summary or overview, the shaping of all the physically applicable properties in a fuel stack system will necessitates agile tools that can integrate multiple physical domains into the same model. Equation-based language and causal modeling capabilities enable physics models. This is very practical when you want to reuse a component in a variety of settings for a range of objectives.





REFERENCES

- [1] A. Haddad, "Nonlinear dynamic modeling of the PEM fuel cell PEM: Application to the regulation of moisture in the electrolyte membrane," *Thesis of the University of Technology of Belfort Montbéliard*, 2009. [Online] Available: <https://tel.archives-ouvertes.fr/tel-00608632>.
- [2] D. L. Damm, and A. Fedorov, "Radiation heat transfer in SOFC materials and components," *Journal of Power Sources*, vol. 143, no. 1-2, pp. 158-165, 2005, doi: 10.1016/j.jpowsour.2004.11.063.
- [3] A. Wood, H. He, T. Joia, M. Krivy and D. Steedman, "Communication Electrolysis at High Efficiency with Remarkable Hydrogen Production Rates," *Journal of Electrochemical Society*, vol. 163, no. 5, pp. 327-329, 2016.
- [4] K. Sedghisigarchi and A. Feliachi, "Dynamic and transient analysis of power distribution systems with fuel Cells-part I: fuel-cell dynamic model," *IEEE Transactions on Energy Conversion*, vol. 19, no. 2, pp. 423-428, 2004, doi: 10.1109/TEC.2004.827039.
- [5] G. Rinaldi *et al.*, "Post-test Analysis on a Solid Oxide Cell Stack Operated for 10,700 Hours in Steam Electrolysis Mode," *Fuel Cells*, no. 17, no. 4, pp. 541-549, 2017, doi: 10.1002/face.201600194.
- [6] D. H. Jeon, "Computational fluid dynamics simulation of anode-supported solid oxide fuel cells with implementing complete overpotential," *Energy*, vol. 188, no. 116050, 2019, doi: 10.1016/j.energy.2019.116050.
- [7] H. Zhang, H. Xu, B. Chen, F. Dong and M. Ni, "Two-stage thermoelectric generators for waste heat recovery from solid oxide fuel cells," *Energy*, vol. 132, pp. 280-288, 2017, doi: 10.1016/j.energy.2017.05.005.
- [8] C. Chatzichristodoulou, M. Chen, P. V. Hendriksen, T. Jacobsen and M. B. Mogensen, "Understanding degradation of solid oxide electrolysis cells through modeling of electrochemical potential profiles," *Electrochimica Acta*, vol. 189, pp. 265-282, 2016, doi: 10.1016/j.electacta.2015.12.067.
- [9] M. Beigzadeh, F. Pourfayaz and M. H. Ahmadi, "Modeling and improvement of solid oxide fuel cell-single effect absorption chiller hybrid system by using nano-fluids as heat transporters," *Applied Thermal Engineering*, vol. 166, no. 114707, 2020, doi: 10.1016/j.applthermaleng.2019.114707.
- [10] Z. Lyu, H. Li and M. Han, "Electrochemical properties and thermal neutral state of solid oxide fuel cells with direct internal reforming of methane," *International Journal of Hydrogen Energy*, vol. 44, no. 23, pp. 12151-12162, 2019, doi: 10.1016/j.ijhydene.2019.03.048.
- [11] D. M. S. Mosqueda, F. E. Blancas, D. Pumiglia, F. Santoni, C. B. Munoz and S. J. McPhail, "Intermediate temperature solid oxide fuel cell under internal reforming: Critical operating conditions, associated problems and their impact on the performance," *Applied Energy*, vol. 235, pp. 625-640, 2019, doi: 10.1016/j.apenergy.2018.10.117.
- [12] V. Subotic *et al.*, "On the origin of degradation in fuel cells and its fast identification by applying unconventional online-monitoring tools," *Appl. Energy*, vol. 277, no. 115603, 2020, doi: 10.1016/j.apenergy.2020.115603.
- [13] T. Theuer, "Sustainable Syngas Production by High-Temperature Co-electrolysis," *ChemieIngenieur Technik*, vol. 92, no. 1-2, pp. 40-44, 2020, doi: 10.1002/cite.201900174.
- [14] H. B. Huo, X. J. Zhu and G. Y. Cao, "Nonlinear modeling of a SOFC stack based on a least squares support vector machine," *Journal of Energy Sources*, vol. 162, no. 2, pp. 1220-1225, 2006, doi: 10.1016/j.jpowsour.2006.07.031.
- [15] J. Milewski and A. Miller, "Influences of electrolyte type and thickness on solid oxide fuel cell hybrid system performance," *Journal of fuel cell science and technology*, vol. 3, no. 4, pp. 396-402, 2006, doi: 10.1115/1.2349519.





- [16] M. Santarelli; P. Léone; M. Calé; G. Orsello, "Experimental evaluation of fuel use and air management sensitivity on a 100 kW SOFC system," *Journal of Energy Sources*, vol. 171, no. 1, pp. 155-168, 2017, doi: 10.1016/j.jpowsour.2006.12.032.
- [17] L. A. Chick, R. E. Williford and J. W. Stevenson, "Spreadsheet Model of SOFC Electrochemical Performance," *SECA modeling & simulation training session August*, 2003.
- [18] Fuel Cell Handbook, "Strategic Center for Natural Gas," 6th edition, U.S. Department of Energy/National Energy Technology Laboratory Morgantown, 2002.
- [19] K. Keegan, M. Khaleel, L. Chick, K. Recknagle, S. Simner, and J. Deibler, "Analysis of a Planar Solid Oxide Fuel Cell Based Automotive Auxiliary Power Unit," *SAE Technical Paper Series*, no. 1-12, 2002.
- [20] J. Larminie and A. Dicks, "Fuel Cell Systems Explained," *John Wiley & Sons Ltd*, The Atrium, Southern Gate, Chichester, West Sussex PO19 8SQ, England, 2003.
- [21] S. C. Singhal and K. Kendall, "High Temperatures Solid Oxide Fuel Cells: Fundamentals, Design and Applications," *Elsevier Ltd, The Boulevard, Langford Lane, Kidlington, Oxford OX5 1GB, UK*, 2004.
- [22] B. R. Joseph, "Optimal Design and Operation of Solid Oxide Fuel Cell Systems for Small-Scale Stationary Applications," *Ph.D. Thesis, University of Wisconsin, Madison, USA*, 2002.
- [23] G. Chen, "Advanced Fuel Cell Based on New Nano crystalline Structure Gd_{0.1}Ce_{0.9}O₂ Electrolyte," *ACS Appl Mater Interfaces*, vol. 11, no. 11, pp. 10642-10650, 2019, doi: 10.1021/acsami.8b20454.
- [24] M. Hauck, S. Herrmann and H. Spliethoff, "Simulation of a reversible SOFC with Aspen Plus," *International Journal of Hydrogen Energy*, vol. 42, no. 15, pp. 10329-10340, 2017, doi: 10.1016/j.ijhydene.2017.01.189.
- [25] S. Amiri, R. E. Hayes and P. Sarkar, "Transient simulation of a tubular micro-solid oxide fuel cell," *Journal of Power Sources*, vol. 407, pp. 63-69, 2018, doi: 10.1016/j.jpowsour.2018.10.062.
- [26] A. Nafees and R. A. Rasid, "Simulation of a Natural Gas Fueled Solid Oxide Fuel Cells TBS," *IOP Conference Series: Materials Science and Engineering*, vol. 702, pp. 1-17, 2019, doi: 10.1088/1757-899X/702/1/012017.
- [27] T. V. V. S. Lakshmi, P. Geethanjali and P. S. Krishna, "Mathematical modelling of solid oxide fuel cell using Matlab/Simulink," *Annual International Conference on Emerging Research Areas and 2013 International Conference on Microelectronics, Communications and Renewable Energy*, 2013, pp. 1-5, doi: 10.1109/AICERA-ICMiCR.2013.6576016.
- [28] R. Kungas, "Review—electrochemical CO₂ reduction for CO production: Comparison of low- and high-temperature electrolysis technologies," *Journal of The Electrochemical Society*, vol. 167, no. 4, pp. 1-12, 2020.
- [29] X. Wang, X. Lv and Y. Weng, "Performance analysis of a biogas-fueled SOFC/gthybrid system integrated with anode-combustor exhaust gas recirculation loops," *Energy*, vol. 197, no. 117213, 2020, doi: 10.1016/j.energy.2020.117213.
- [30] M. Mankour, M. Sekour, A. Hamlet and M. Fourali, "Characterization and Simulation of Solid Oxide Fuel Cell (SOFC)," *Lecture Notes in Networks and Systems book series*, LNNS, vol. 361, 2021.
- [31] Y. Song, X. Zhang, K. Xie, G. Wang and X. Bao, "High-temperature CO₂ electrolysis in solid oxide electrolysis cells: Developments, challenges, and prospects," *Advanced Materials*, vol. 31, no. 50, pp. 1-18, 2019, doi: 10.1002/adma.201902033.
- [32] J. Sihvo, T. Roinila and D. -I. Stroe, "Novel Fitting Algorithm for Parametrization of Equivalent Circuit Model of Li-Ion Battery From Broadband Impedance Measurements," *IEEE Transactions on Industrial Electronics*, vol. 68, no. 6, pp. 4916-4926, 2021, doi: 10.1109/TIE.2020.2988235.
- [33] M. Zic, I. Fajfar, V. Subotic, S. Pereverzyev and M. Kunavar, "Investigation of Electrochemical Processes in Solid Oxide Fuel Cells by Modified Levenberg–Marquardt Algorithm: A New Automatic Update Limit Strategy," *Processes*, vol. 9, no. 1, pp. 1-14, 2021, doi: 10.3390/pr9010108.
- [34] M. Mankour and M. Sekour, "Modeling of Fuel Cell SOFC," *International Conference in Artificial Intelligence in Renewable Energetic Systems*, 2019, pp. 471-482, doi: 10.1007/978-3-030-04789-4_50.
- [35] M. Mankour, M. Sekour, and L. Boumadien, "Thermal Characterization of a SOFC Fuel Cell," *International Conference in Artificial Intelligence in Renewable Energetic Systems*, 2020, pp. 930-936, doi: /10.1007/978-3-030-63846-7.

BIOGRAPHIES OF AUTHORS



Mankour Mohamed     was born in Saida (Algeria), in 1977. He obtained a diploma of engineer in Electrotechnical in 2003. He received his master degrees in materials electrical engineering from Science and technology university Oran, Algeria, in 2006. In September 2006, he joined the science and technology university, Oran, Algeria. Where he worked on modeling glow discharges controlled by dielectric barrier. He received the degree of "Doctor at Es-Science" in modeling glow discharges controlled by dielectric barrier at 2014. He received the degree of HDR at the University of Saida in 2017, His fields of interest include renewable energy, Fuel Cell, plasma physics and materials. He is member and team leader in Electrotechnical Engineering Laboratory (L.G.E) electrical engineering. He can be contacted at email: mankoumohamed312@yahoo.fr.



Sekour M'hamed     was born in Saida (Algeria) in 1964. He received my Master in 2007 at the ENSET Oran. He received the degree of "Doctor at Es-Science" in Electrical Control from the same institution in 2013. He is currently an Associate Professor at the University of Saida. His fields of interest include multimachine multi-converter systems, power electronics and optimization of renewable energy system. His current activities include works on smart grid and energy storage systems. He received the degree of HDR at the University of Saida in 2018. He is member and team leader in Electrotechnical Engineering Laboratory (L.G.E). He can be contacted at email: sekourmohamed@yahoo.fr.